

Report for AOARD 10-4139, 11-4099 & 12-4067  
“Ion Source Development for a Compact Proton Beam Writing System III”

28 June 2013

JA van Kan<sup>1</sup>, C.W. Hagen<sup>2</sup>, T. Osipowicz<sup>3</sup>, A. Khursheed<sup>4</sup> and F Watt<sup>5</sup>

<sup>1</sup>Associate Professor of Physics, NUS, Singapore\*.

<sup>2</sup>Faculty of Applied Sciences, Delft University of Technology, Lorentzweg 1, 2628CJ Delft,  
The Netherlands

<sup>3</sup>Director of CIBA, Deputy head of Physics and Assoc. Professor of Physics, NUS,  
Singapore\*.

<sup>4</sup>Assoc. Professor in the Electrical Engineering Department, NUS, Singapore

<sup>5</sup> Professorial Fellow of Physics, NUS, Singapore\*.

\*Centre for Ion Beam Applications (CIBA) Physics Department, Faculty of Science,  
National University of Singapore (NUS), 2 Science Drive 3, Singapore 117542

**Dr Jeroen A van Kan:**

- e-mail address : [phyjavk@nus.edu.sg](mailto:phyjavk@nus.edu.sg)
- Institution : CIBA, Physics Department, NUS
- Mailing Address : 2 Science drive 3, 117542 Singapore
- Phone : +65 6516 6978
- Fax : +65 6777 6126

Period of Performance: 22/07/2010 – 20/06/2013 (grants: 10-4139, 11-4099 & 12-4067)

**Abstract:**

During this contract period the PI, a PhD student, a research fellow, a research technician and the collaborators have been working on this project. During the field trips to Delft University the team has gained valuable knowledge and have achieved the first results with the electron-impact ion source system. Through this exchange the team has now a realistic design for the ion source test bench which has produced its first beams at 3 keV and is currently being tested in Singapore. In a next stage this system will be employed at ion energies of up to 200 keV.

Electron beam calculations have been performed to evaluate different electron guns for their effectiveness in ionizing hydrogen gas molecules in our proposed configuration. Our calculations show that the proposed PBW system is expected to write as fast as commercial electron beam writing systems at sub 10 nm, without proximity effects from nearby fabricated features. Several electron impact ionization chips have been designed and tested in Delft and Singapore.

At the same time the new proton beam writing beam line developed under grants AOARD 07-4017 & 09-4020 has been further improved and proton beams can now be focused down to  $13 \times 29 \text{ nm}^2$ .

## Report Documentation Page

*Form Approved*  
OMB No. 0704-0188

Public reporting burden for the collection of information is estimated to average 1 hour per response, including the time for reviewing instructions, searching existing data sources, gathering and maintaining the data needed, and completing and reviewing the collection of information. Send comments regarding this burden estimate or any other aspect of this collection of information, including suggestions for reducing this burden, to Washington Headquarters Services, Directorate for Information Operations and Reports, 1215 Jefferson Davis Highway, Suite 1204, Arlington VA 22202-4302. Respondents should be aware that notwithstanding any other provision of law, no person shall be subject to a penalty for failing to comply with a collection of information if it does not display a currently valid OMB control number.

1. REPORT DATE <b>05 AUG 2013</b>	2. REPORT TYPE <b>Final</b>	3. DATES COVERED <b>22-05-2012 to 21-05-2013</b>			
4. TITLE AND SUBTITLE <b>Ion Source Development for a Compact Proton Beam Writing System III</b>		5a. CONTRACT NUMBER <b>FA2386-12-1-4067</b>			
		5b. GRANT NUMBER			
		5c. PROGRAM ELEMENT NUMBER			
6. AUTHOR(S) <b>Jeroen van Kan; C Hagan; T Osopowicz; A Khursheed; F Watt</b>		5d. PROJECT NUMBER			
		5e. TASK NUMBER			
		5f. WORK UNIT NUMBER			
7. PERFORMING ORGANIZATION NAME(S) AND ADDRESS(ES) <b>CIBA, Physics Department, ,National University of Singapore,2 Science Drive 3, 117542,Singapore,NA,NA</b>		8. PERFORMING ORGANIZATION REPORT NUMBER <b>N/A</b>			
9. SPONSORING/MONITORING AGENCY NAME(S) AND ADDRESS(ES) <b>AOARD, UNIT 45002, APO, AP, 96338-5002</b>		10. SPONSOR/MONITOR'S ACRONYM(S) <b>AOARD</b>			
		11. SPONSOR/MONITOR'S REPORT NUMBER(S) <b>AOARD-124067</b>			
12. DISTRIBUTION/AVAILABILITY STATEMENT <b>Approved for public release; distribution unlimited</b>					
13. SUPPLEMENTARY NOTES					
14. ABSTRACT <b>Through a technical exchange with Delft University, the NUS research team has gained valuable knowledge and have achieved the first results with the electron-impact ion source system. Through this exchange, the team has achieved a realistic design for the ion source test bench which has produced is first beams at 3 keV and is currently being tested in Singapore. In a next stage, this system will be employed at ion energies of up to 200 keV. Electron beam calculations have been performed to evaluate different electron guns for their effectiveness in ionizing hydrogen gas molecules in our proposed configuration. Our calculations show that the proposed PBW system is expected to write as fast as commercial electron beam writing systems at sub 10nm, without proximity effects from nearby fabricated features. Several electron impact ionization chips have been designed and tested at Delft and Singapore. At the same time, the new proton beam writing beam line developed under previous grant efforts has been further improved and proton beams now can be focused to 13nm x 29nm.</b>					
15. SUBJECT TERMS <b>Proton Beam Writing, Electron Gun, Ion Source, Ion Source Test Bench</b>					
16. SECURITY CLASSIFICATION OF:			17. LIMITATION OF ABSTRACT <b>Same as Report (SAR)</b>	18. NUMBER OF PAGES <b>24</b>	19a. NAME OF RESPONSIBLE PERSON
a. REPORT <b>unclassified</b>	b. ABSTRACT <b>unclassified</b>	c. THIS PAGE <b>unclassified</b>			



## **Introduction: Current status**

To overcome the diffraction constraints of traditional optical lithography, the next generation lithographies (NGLs) will utilize any one or more of EUV (extreme ultraviolet), X-ray, electron or ion beam technologies for producing sub-100nm features.

Electron beam lithography (EBL), a candidate for direct-write technology at nanodimensions has extensively been investigated for the last four decades. However, high resolution lines and spaces in single step exposures for EBL are limited to about 20-30 nm levels due to proximity effects from high energetic secondary electrons initiating from adjacent and nearby features giving rise to structure broadening.

Perhaps the most under-developed and under-rated is the utilisation of ions for lithographic purposes. The three ion beam techniques, Proton Beam Writing (PBW), Focused Ion Beam (FIB) and Ion Projection Lithography (IPL) have the flexibility and potential to become leading contenders as NGLs [1]. Since the introduction of PBW in the Japanese governments road map for the nanotechnology business creation initiative (see appendix I) a large multinational corporation, Kobelco, has been pushing the development of compact accelerators for PBW applications. The Shibaura Institute of Technology (Tokyo, Japan) has recently received a 2M US\$ grant from the Japanese government to develop PBW. In our Centre for Ion Beam Applications (CIBA), Physics Department, National University Singapore *we established sub 100 nm proton beam focusing for protons down to  $35 \times 75 \text{ nm}^2$  [2] and have produced 3D high aspect ratio walls down to 22 nm in HSQ [3]*. The minimum obtainable feature size is expected to be in the nano meter range, due to the absence of proximity effects. In order to achieve nm sized features the proton probe has to be focused down to nm dimensions.

In CIBA we have been working on next generation systems for proton beam focusing. The success of a next generation PBW system depends on two main components: a **stable high brightness source of MeV protons** and a **high quality focusing lens system**. With the help of the US air force we have designed a new system for proton beam writing (AOARD 07-4017). The key characteristics are an improvement of the system demagnification. In initial experiments a beam has been focused down to 13 nm in x direction, closely matching the beam optical calculations.

Proton beam writing has the advantage of proximity free fabrication of high aspect-ratio nanostructures in photo-resist. Recently a proton beam size of  $13 \times 30 \text{ nm}^2$ , has been achieved at a current of about 4 fA. The reduced brightness was measured to be about  $10 \text{ A/m}^2 \text{ SrV}$  [4]. For proton beam writing, the exposure dosage for photo-resist is typically  $10\text{-}100 \text{ nC/mm}^2$ . The beam resolution and writing time are limited by the low brightness RF ion source.

## **Experiment, Results and Discussion:**

### **Ion source test bench setup**

With the goal of enhancing the performance of RF ion source used in the CIBA Singletron accelerator, we have engaged in constructing an ion source test bench, which is expected to improve the ion source brightness by about 10 times. This basic test setup will comprise of a gas handling system, high voltage and RF power supply to ionize the hydrogen gas molecules. The system will eventually be able to measure the proton beam current, energy spread and brightness. Initially the system will be tested at low voltage (several kV). The test-bench schematics are shown in Fig. 1. Later the test bench (Fig. 2) will be upgraded to operate at about 200 kV, which will potentially be used as a compact PBW system.

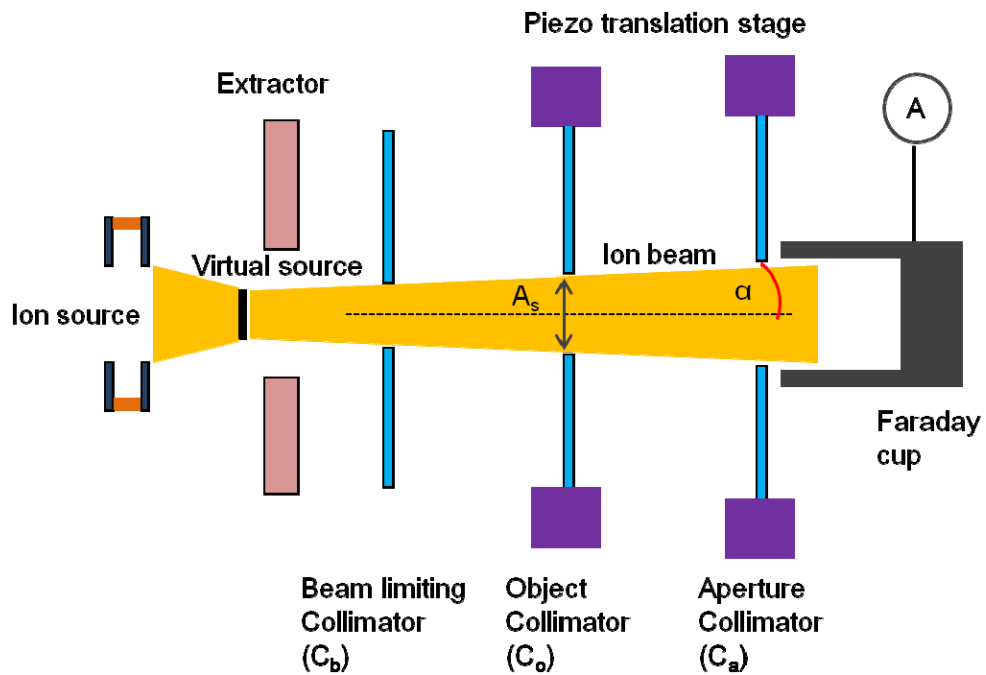


**Figure 1.** Schematics of Ion-Source test bench and Brightness Measurement setup.

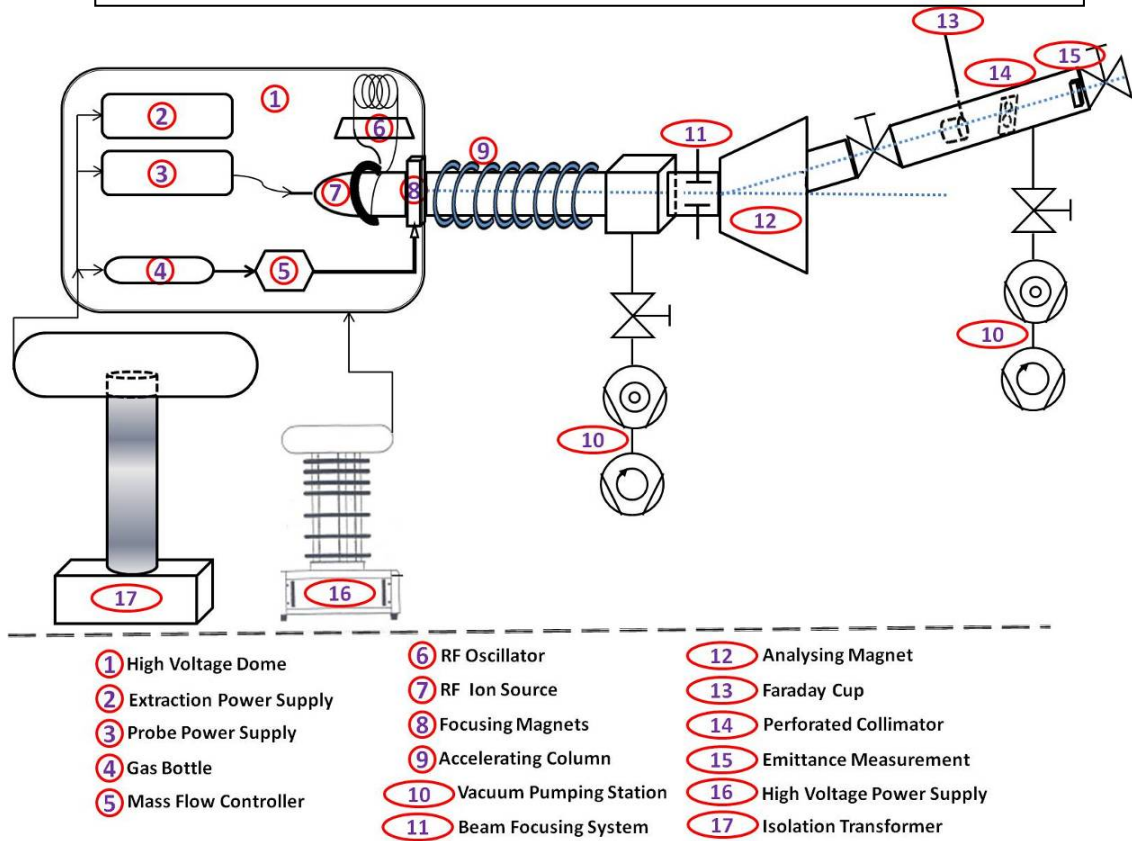


**Figure 2:** Schematic diagram of Ion-Source Test Bench along with the low energy ion accelerator set-up, possibly can be used as compact PBW system.

## Ion source characterization setup

We are currently developing the ion beam diagnostic tools to be integrated into the test bench and the SEM chamber. They are the beam brightness measurement tool and beam energy spread analyzer.

The beam brightness measurement tool consists of 3 sets of collimators ( $C_b$ ,  $C_o$  and  $C_a$ ) out of which two ( $C_o$  and  $C_a$ ) will be installed on (piezo) translation stages (Fig. 1). By controlling the piezo translation stage, the opening size of the objective and aperture collimators can be adjusted with accuracy of 20 nm in case of the electron impact ion source (NAIS). In the RF ion source test set-up relatively coarse control of the apertures with manual stages is sufficient. Using the 2-slit method, the objective collimator open size  $A_s$  and the beam half divergence  $\alpha$  are known. The ion beam current  $I_p$  can be measured by a Faraday cup and picoamp-meter. Therefore the ion beam/ source reduced brightness can be estimated as Eq. (1), where  $V$  is the ion beam energy in eV.

$$B_r = \frac{I_p}{A_s \Omega V} = \frac{I_p}{A_s \pi \alpha^2 V} \quad (1)$$

The beam energy spread diagnostic setup is based on Einzel electrostatic retarding field analyzer [5] (Fig. 3). By varying the potential of the retarding electrode (accuracy of 0.1 V), the ions are selectively collected by the Faraday cup, according to their energy. The ion beam energy profile can then be obtained, with a differential plot of the ion current versus the retarding electrode potential.

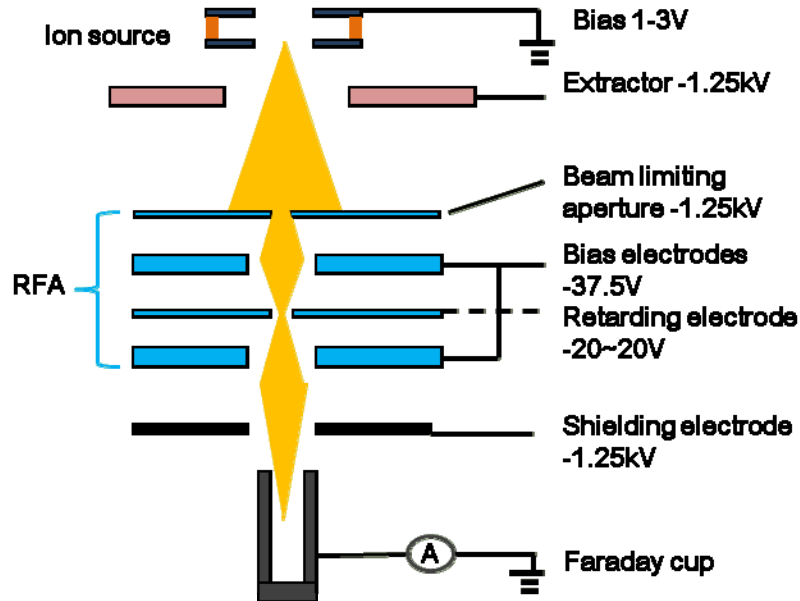


*Figure 3: Proposed ion beam energy spread measurement setup.*

The characterization results of RF and electron impact gas ion source (ion beam current, reduced brightness and energy spread) will be examined with the above diagnostic tools and cross-checked with the theoretical prediction.

## Present Ion-Source Test Bench Set-up at CIBA

Figure 4 shows a photograph of the ion-source test bench set up at CIBA, NUS.

### Actual photograph of Ion Source Test Bench for B<sub>r</sub> Measurements

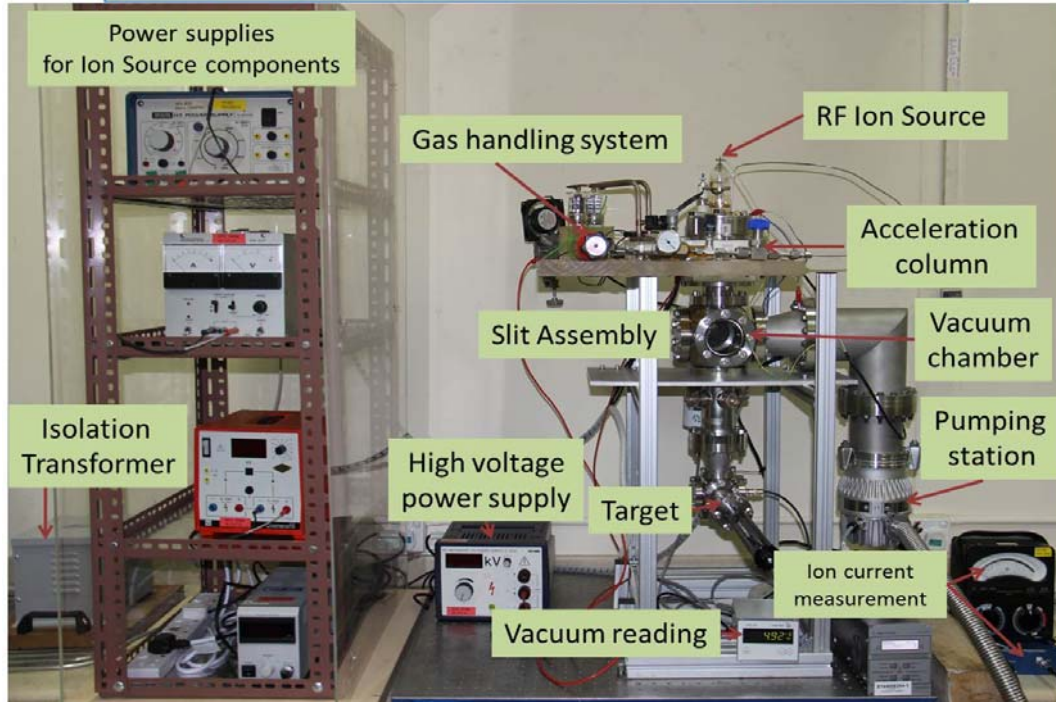


**Figure 4:** Photograph of the existing ion source test setup. In the left: isolation transformer and the power supplies for ion source components, on the center: high voltage power supply, on the right top: RF Ion Source, gas handling system and accelerating column, on the right bottom: the slit assembly, vacuum chamber with target (where ion current is measured), current integrator and the pumping system.

Improving from our old set-up, the present ion-source test bench now has the capability to operate at high voltages (upto 250 kV). Necessary arrangements for measuring the beam brightness ( $B_r$ ) are also in place. Since the procurement and installation of a high voltage isolation transformer (withstanding a voltage separation of about 250 kV) is under processing, we currently run the RF ion source, in the test bench, to yield ion beam with energies up to 3 keV.

The electrical power required to operate multiple components (like RF Valve, Probe and Extraction voltages) on the Ion Source were provided by appropriate power supplies. Since the whole Ion Source assembly has to be elevated to a very high potential (upto to about 200 kV) during operation, the power supplies which feed power to different components of Ion Source also need to be insulated from the ground potential. This is achieved by (i) strategically placing those power supplies in a Perspex box (as seen on the left side of Fig. 4), and (ii) they are powered through an isolation transformer. The required gas, to be ionized in the RF ion source, is fed through a coarse needle valve regulator (marked as *Gas handling system* in Fig. 4). An oscillating RF voltage, operated at around 100 MHz, is capacitatively coupled onto the gas filled quartz tube (marked as *RF Ion Source* in Fig. 4). The plasma, inside the quartz tube, is generated by the coupling of RF power of a few hundred watts to a gas at a pressure of  $10^{-4}$  to  $10^{-5}$  mbar (as measured in the *vacuum chamber*). The plasma is biased positively (through *probe voltage* as shown in Fig. 5) relative to the extraction canal and the ions are extracted through the narrow canal, with

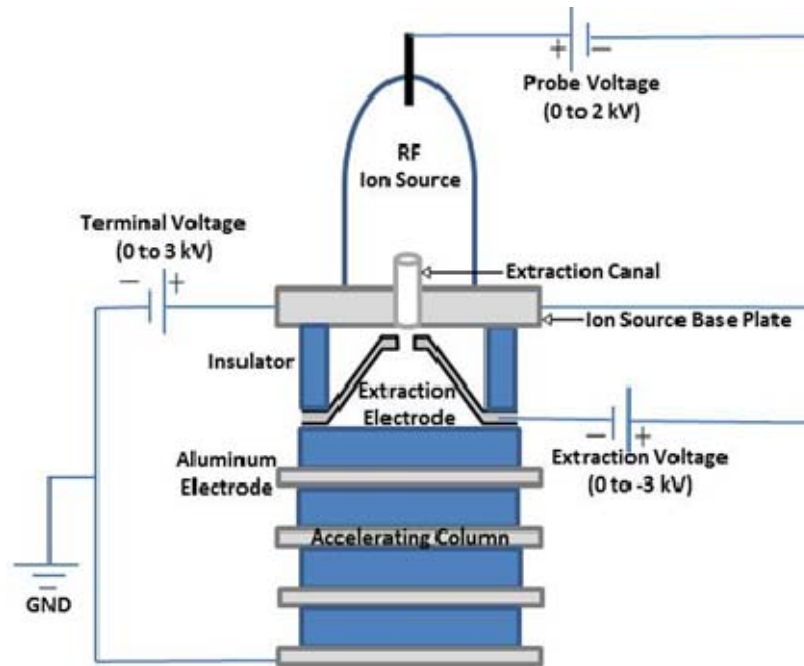


**Figure 5: Schematic diagram describing the electrical connections on the Ion-Source Test Bench set-up**

a variable extraction voltage of 0 to -3 kV. The detailed electrical connections are schematically described in Fig. 5. The whole assembly (ion source, power supplies, RF generator etc.) is housed in an insulated enclosure, which is elevated to the required high voltage (Terminal Voltage), generated by a 3 kV solid-state power supply (marked as *High voltage power supply* in Fig. 4). The extracted beam is accelerated in a column, made from a series of aluminum electrodes separated by insulating rings (marked as *Acceleration column* in Fig. 4). A constant potential drop is maintained across each electrode, through an appropriate resistor arrangement, the accelerated ions will reach ground potential on the last electrode.

Three set of slits have been incorporated in the Ion Source test-bench set up (marked as *Slit Assembly* in Fig. 4). These slit assemblies will be used, in combination with the ion current measurements system (using *Charge Integrator*), to evaluate the brightness of the ion beam ( $B_r$ ). These slits were fabricated in-house with the existing techniques (explained in detail later). The high energy beam exiting from the accelerating column will initially pass through a stainless steel slit of 2 mm diameter (marked as  $C_b$  in Fig. 1). After this, the well-defined beam will be collimated using two set of fine-slits (marked as  $C_o$  and  $C_a$  in Fig. 1), with opening sizes ranging from 100  $\mu\text{m}$  to 1000  $\mu\text{m}$ . The ion beam after passing through this slit assembly will be collected onto a target (marked as *Target* in Fig. 4) and ion current will be measured (marked as *Ion Current Measurement* in Fig. 4).

### Slits fabrication for $B_r$ measurements in the RF ion source

There are three set of slits ( $C_b$ ,  $C_o$  and  $C_a$ ) used in this Ion Source test bench set-up enabling to measure the ion beam brightness. The first slit  $C_b$  is made out of a 1 mm thick stainless steel with 2 mm diameter opening. This slit is placed at the exit of accelerating column. The other slits ( $C_o$  and  $C_a$ ) were fabricated in a 20  $\mu\text{m}$  thick Ni foil through UV lithographic and electroplating technique in CIBA, NUS, and are schematically described

in Fig. 6a. The photograph of the final fabricated Ni slits is shown in Fig. 6b along with a 10 cent coin for size comparison. The systematic steps involved in fabricating these slits are as follows:

The fabrication process of the Ni slits involves several key steps, listed in Fig. 6. Firstly, the substrate is prepared by sputtering of Cr and Cu seed layers onto a piece of silicon wafer. This is followed by spin coating of AR-p positive photoresist and UV lithography using a photo mask which has been made using a Laser Writer in CIBA, NUS. The exposed AR-p is then developed by immersing in AR300-26 solution. The resulting substrate is then electroplated with nickel, followed by removing of the residual photoresist. The final Ni slits with appropriate openings ( $C_o$ : 250, 500 and 1000  $\mu\text{m}$  and  $C_a$ : 100, 250 and 500  $\mu\text{m}$  openings) are then obtained by etching away the Cu seed layer.

*Step 1: Magnetron sputtering of seed layer*

Cr (5 nm) and Cu (50 nm) seed layers are sputtered on a silicon wafer. The Cr layer was added to enhance the adhesion of the Cu layer to the Si substrate. The Cu layer provides the conductivity required for the electroplating. Moreover, the Cu layer can also be easily etched using sodium persulfate without damaging the electroplated Ni layer.

*Step 2: Spin coating of AR-p photoresist layer.*

A positive photoresist AR-p 3210 is spin coated on Cu/Cr/Si substrate using a three step approach. Low starting spin speed (30 s) is followed by a main spin speed of 900-1700 rpm, for 2 minutes 15 seconds. Marginal beads are reduced by a final spin rotation at 800 rpm for 5 seconds. The resulting spin coat layer is prebaked at 95 °C for 10 minutes to reduce the remaining solvent content to improve the resist adhesion to the substrate and avoid mask contamination and/or sticking to the mask during UV lithography.

*Step 3: UV lithography and Development of pattern*

With the photoresist layer, UV lithography is then used with the made photo mask to create the aperture array pattern on the photoresist. The exposed AR-p is then developed with AR300-26 developer diluted in DI water (1:3 ratio) for 1 min followed by a DI water rinse and dried with an air gun. There is a need to minimise the development time to prevent the pillars from deforming or collapsing. Post-development baking of 110 °C improves adhesion and resistance of the structure during the electroplating and developing process.

*Step 4: Electroplating of nickel and Removal of residual photoresist*

With the AR-p pillars, nickel plating can then be used to form the Ni slits with appropriate openings in it. A 20  $\mu\text{m}$  Ni layer was electroplated with a plating rate of 0.5  $\mu\text{m}/\text{min}$ . The residual AR-p was then removed by acetone in an ultrasonic bath for 1 min.

*Step 5: Etching of Cu seed layer*

As a last step of the fabrication process, the etching of Cu seed layer was carried out to lift off the Ni slits from the substrate. This is done by immersing it in a solution of 60 grams of sodium persulfate mixed with 40 ml DI water. The solution is kept at 45 °C until the nickel foil has been separated from the silicon substrate. The nickel foil is then rinsed with DI water and dried using an air gun.

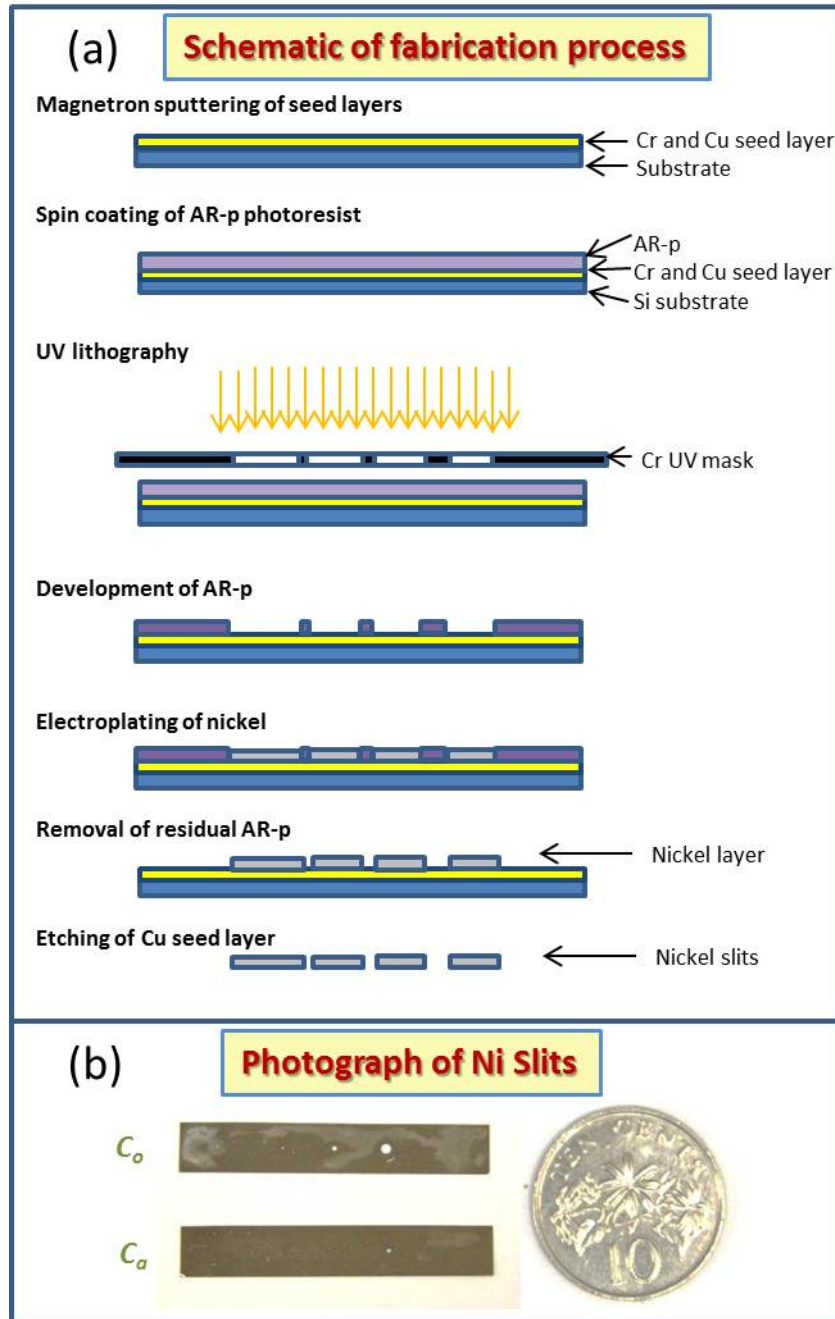


**Figure 6:** (a) Schematic of Ni Slit fabrication process and (b) Photograph of Ni slits, with 10 cents coin for size comparison.

As a trial run, we managed to operate the ion source and produce nitrogen ions with energy of 2 keV from this test bench set-up. Initially, the potential of the ion-source assembly was raised to about 2 kV with the help of the 3 kV isolation transformer. Further to this process, the amount of gas fed, RF power and probe voltage were remotely adjusted, using a fiber optic communication system (will be described in detail at later section), to an optimal value to form the plasma in the ion-source quartz tube. The pressure of such stable plasma was maintained at around  $1.5 \times 10^{-6}$  mbar (as measured in the *vacuum chamber*). Then the positive ions from the ion source were extracted by negatively biasing the plasma

with -1 kV. Currently the accelerating column only serves as a drift tube for these extracted 2 keV  $N^+$  ions. The ion current of 2 keV  $N^+$  ions was measured to be around 350 nA on a conductive copper plate, positioned at the point *Target* in Fig. 4.

In the near future we will use this system to measure the ion beam brightness ( $B_r$ ). With beam brightness measurement, the high energy ions will be subjected to various beam characterization to quantify the performance of RF ion-source. This set-up will further allow us to optimize different ion-source parameter (RF Ion Source: RF power, Gas pressure, Ion-Source Geometry, Probe Voltage, Extraction Voltage etc.) to obtain higher beam brightness. In a follow up experiment this test-bench will be adopted to evaluate the performance of the electron impact ion source (NAIS, see progress below).

### **Fiber optic communication system**

During the operation of the ion-source, as stated above, the whole ion-source assembly will be elevated to high potential (~100 kV). With such a large potential difference on this isolated assembly, it becomes lethal for an operator to touch-and-operate the appropriate components. But in practice, to obtain an optimal ion current, the ion-source parameters (RF power, probe voltage, extraction voltage etc.) has to be tuned dynamically. With diligent effort, a solution to this constrain was achieved by controlling the high voltage components remotely using the fiber optic communication system. Figure 7 shows the schematic view of the fiber optic communication system adopted to control the individual components, at the high voltage terminal, remotely in our test-bench setup at CIBA, NUS. The computer codes were developed using Labview Control VI programs to control and diagnose the input and output signals to these components. The combination of two USB extender (local and remote) system (Make: ICRON, Model: USB Ranger<sup>®</sup> 2224) were used to communicate the required signal from the computer to the data acquisition (DAQ) card (Make: National Instruments, Model: NI-USB-6211) at the high voltage terminal. The communication between the USB extender at the ground terminal and high voltage terminal was achieved through a long Duplex LC connector fiber optic cable. The signal reaching the remote USB extender, via optic fiber, is then fed to the DAQ card, which controls the individual high voltage power supplies (like RF power, probe voltage, extraction voltage etc.). The present remote USB extender system has the capability to control four different DAQ cards independently, and each DAQ (NI-USB-6211) can control two power supplies simultaneously, thus enabling to control eight power supplies in total at the high voltage terminal. Here in our trial run, we demonstrated the successful operation of probe voltage power supply, at high voltage terminal, using this remote control fiber optic system. With the ion-source assembly elevated to a higher potential of 2 kV, the probe voltage was varied, remotely, between 50 and 500 V using this fiber optic communication system. The increase in probe voltage had a corresponding effect on the extracted ion current (increased from 75 nA to 350 nA). This accomplished methodology used in remote controlling the probe voltage will later be extended to operate other power supplies located at the high voltage terminal, enabling us to obtain an optimal ion current and brightness from the RF ion source.

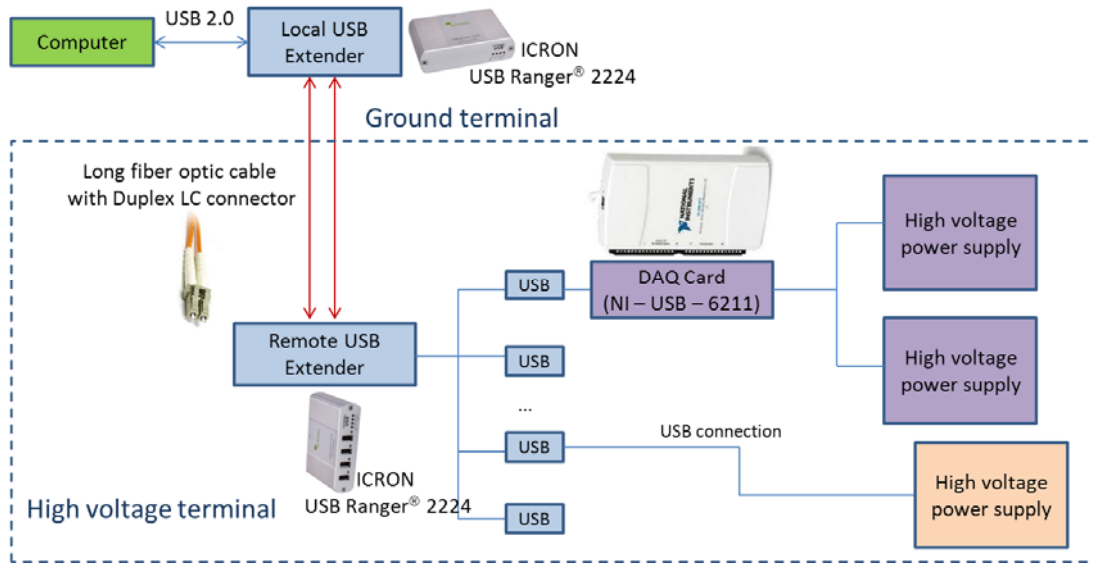


**Figure 7:** Schematic of fiber optic communication system used to control the components, at the high voltage terminal, remotely in the ion-source test bench setup at CIBA, NUS.

### The electron impact gas ion source – concept of NAIS

The electron impact gas ion source that is being developed to improve the brightness for MeV proton beam writing applications will be an alternative for the radio frequency (RF) ion sources that are commonly used to provide proton and helium ion beams for lithography and nuclear microscopy applications in MeV accelerators.

The electron impact gas ion source named Nano Aperture Ion Source (NAIS) designed in Delft is expected to give much higher reduced brightness, about  $10^7$  A/m<sup>2</sup>SrV. Prototypes of the new ion source have been fabricated and tested using a Schottky electron source as injector, by Prof Kruit, Prof Hagen and a PhD student in Delft. The idea of NAIS is to introduce an electron beam into a gas chamber through a double-aperture (0.1 to 1 μm diameter). The gas chamber is miniaturized to provide a small ionization path (0.1 – 10 μm). Once ions are produced inside the gas chamber by electron impact, ions can be extracted by applying a small bias voltage across the gas chamber (see Fig. 8), then extracted by the electric field from an extractor. The channel for gas feeding is fabricated on Si wafers and the sealing was by bonding two Si wafers with glue. The gas feeding window and double-aperture were then created using FIB milling. The NAIS chip encountered membrane deformation during operation and has difficulty to further reduce the space between the two membranes. Therefore to obtain a higher brightness ion beam, a modified version of NAIS chip has been fabricated and under test in TUDelft and NUS.

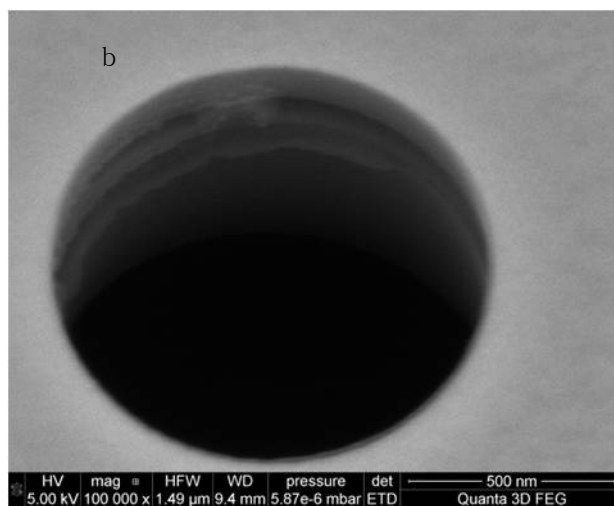
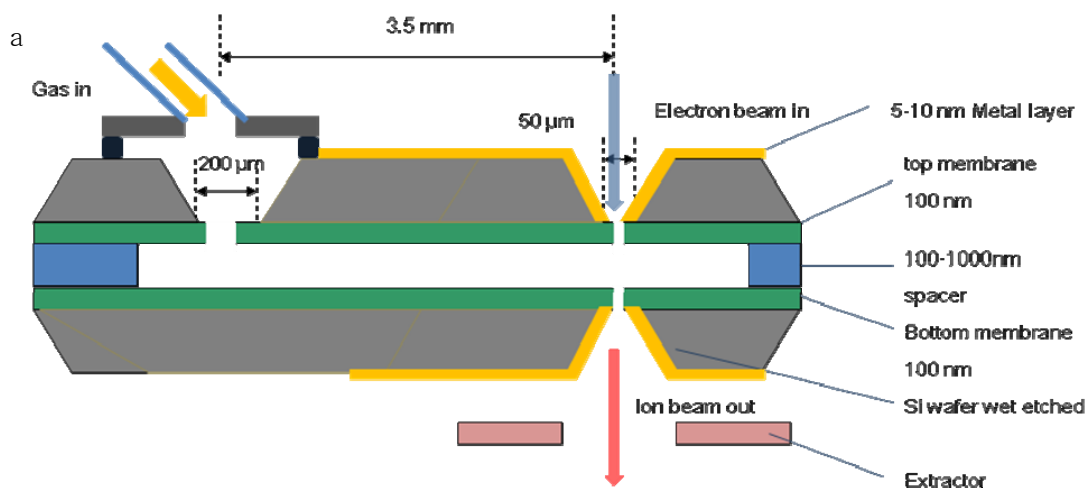


**Figure 8:** NAIS on a silicon chip. a) A narrow channel path for gas is created by depositing thin membranes on Si. Two entrances of 50  $\mu\text{m}$  and 200  $\mu\text{m}$  for beam transport and gas inlet are created respectively. b) High magnification of 900 nm apertures surrounding the gas ionization chamber.

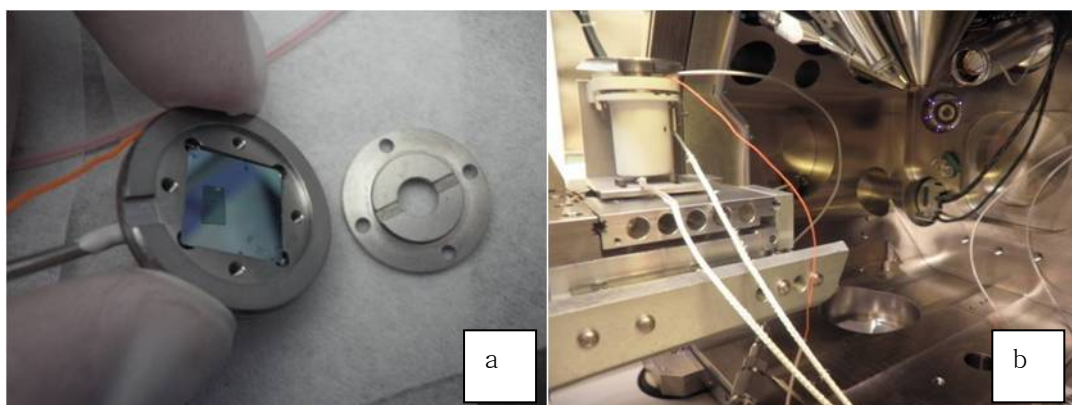


**Figure 9:** a) NAIS gas chamber in sample holder; b) gas chamber mounted in sample holder and sits on SEM stage in chamber (Delft).

Fig. 9 shows the test setup with the NAIS chip mounted in the sample holder (Delft test setup). The NAIS gas chamber is sitting in a SEM chamber, where an electron beam is introduced into the gas chamber to bombard the gas particles for ionization. The induced ion beam current and brightness depend on a few parameters that can be varied for test, which includes the gas feed-in pressure, the bias voltage between the two membranes in the gas chamber, the electron energy and electron beam current.

The experiments have shown an ion beam current of 100-200 pA [6] can be easily achieved. A first theoretical calculation shows the ion beam brightness is comparable to a conventional Gallium Liquid Metal Ion Source (LMIS) for Focused Ion Beam (FIB). With a 1 keV electron beam, the extracted ion currents for helium, air, argon and xenon gases have been obtained and are shown in Fig. 10 as functions of gas inlet pressure.

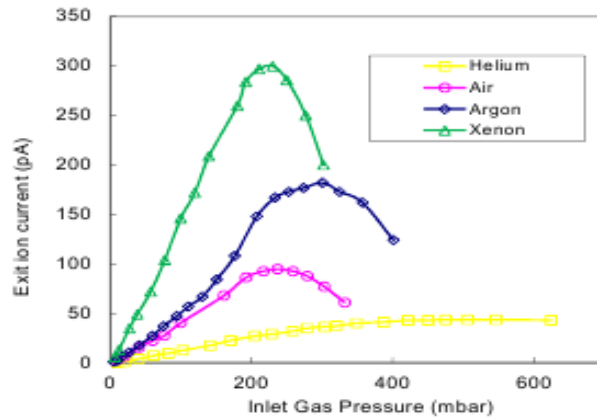


**Figure 10:** The ion beam current outputs from the NAIS source with different gases. At an electron current of 14 nA the ion current varies as a function of pressure and ion type. The current drops with higher gas pressure due to the reduced mean free path.

### The electron impact gas ion source – calculation for a compact high brightness PBW

The ion beam current is a function of the electron current, ionization path length and electron ionization cross-section. The ion beam reduced brightness therefore depends on the **gas ionization chamber geometry**, ion type, electron beam energy and **brightness**. Our current focus is on the theoretical evaluation of conventional electron emitters as injector for this electron impact gas ion source and the gas ionization chamber geometry. We are comparing tungsten hair-pin, LaB6 and Schottky electron sources with hydrogen gas for 10 nm to 10 μm aperture sizes and 100 nm to 1 μm ionization path length (ie membrane spacing). Increasing the path length will yield higher ion current densities at the expense of ion energy spread. The electron beam is optimized for maximum current density in the chamber by considering the electron source brightness and system optical aberrations, without including coulomb interactions [7]. Fig. 11 shows the calculated ion beam reduced brightness as a function of aperture size.

The proposal of a compact high brightness PBW system is based on the current 2<sup>nd</sup> generation PBW beam line at CIBA, NUS [4]. To achieve writing speeds comparable to commercial EBL systems, we aim for a proton beam current of 1 pA with a beam reduced brightness of  $0.2-5 \times 10^6$  A/m<sup>2</sup>SrV. Protons from the NAIS ion source will be accelerated up to 200 keV and focused in the target chamber using either a spaced Russian quadruplet lens configuration or a Spaced triplet lens configuration.

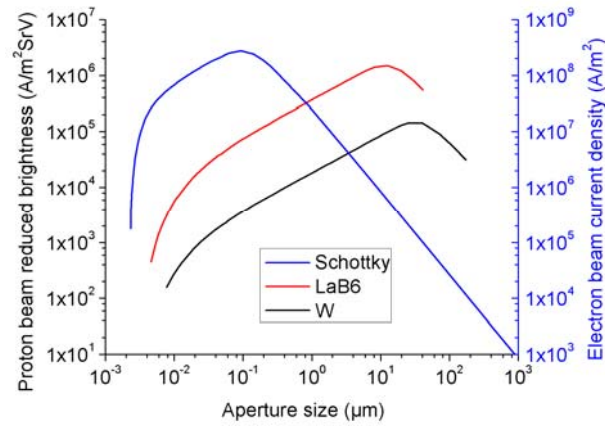


**Figure II:** Ion reduced brightness of hydrogen gas with tungsten hair-pin, LaB6 and Schottky electron sources as a function of aperture size. The ionization path length is 100 nm and the electron beam energy is 1 keV.

**Table 1:** Summary of the ionization chamber designs using a 1 μm path length and listed specifications for a 200 keV PBW system using Tungsten hair-pin, LaB<sub>6</sub> and Schottky electron injectors, with effects of Coulomb interactions included.

Injector	Schottky-injector			LaB6-injector		W-injector	
Gas inlet pressure (mbar)	120			120		120	
Gas leakage rate (mbar l/s)	$2.5 \times 10^{-10}$			$1.0 \times 10^{-9}$		$1.0 \times 10^{-9}$	
Chamber Aperture Diameter (nm)	60	60	200	60	200	60	200
Lens configuration	Russian Quadruplet	Spaced Triplet	Spaced Triplet	Russian Quadruplet	Spaced Triplet	Russian Quadruplet	Spaced Triplet
Proton beam size (nm <sup>2</sup> )	9.5 × 9.5	4.0 × 8.6	8.7 × 12.7	7.5 × 7.5	3.0 × 9.7	7.0 × 7.0	2.5 × 9.5
Proton beam current from ion source (pA)	600	600	3000	12	300	0.6	12
Proton beam current on image plane (pA)	0.2	0.2	0.1	0.005	0.1	0.0005	0.004
Proton beam reduced brightness (A/m <sup>2</sup> SrV)	$1 \times 10^6$	$1 \times 10^6$	$5 \times 10^5$	$3 \times 10^4$	$1 \times 10^5$	$3 \times 10^3$	$5 \times 10^3$

The design of the ionization chamber for the three electron injectors of the electron impact gas ion source includes a few parameters e.g. path length, gas pressure and ionization chamber dimensions. The ionization path length is proposed to be as 1 μm with an inlet gas pressure of 120 mbar for all the three electron injectors (see Table 1). The output proton beam current is maximized avoiding ion-gas molecule collisions. The gas

leakage through this ionization chamber is on the order of  $10^{-10}$  -  $10^{-9}$  mbar l/s. Comparing the three electron injectors, the Schottky electron column shows the greatest potential for a high brightness ( $2.5 \times 10^6$  A/m<sup>2</sup>SrV) and high beam current (0.1-0.2 pA) for fast PBW. The effects of coulomb interactions on the beam spot size are estimated for this system. The trajectory displacement due to coulomb interactions is about 2 nm at the target plane, indicating the possibility of achieving sub-10 nm proton beam. We used Particle Beam Optics Laboratory 3.0 (PBO Lab) simulation to find an optimal quadrupole lens configuration and beam spot size. Simulation result shows that the beam from an aperture of 60 nm can be demagnified down to  $4.0 \times 8.6$  nm<sup>2</sup> by the Russian quadruplet configuration in X and Y direction (Full Width containing 90% of the total beam current). Similarly a beam from a 200 nm aperture can be focused down to  $3.0 \times 9.7$  nm<sup>2</sup> using the spaced triplet configuration in X and Y direction. The outcome of the calculations and simulations of compact PBW systems using the three electron injectors are summarized in Table 1. The performance of a PBW system using a NAIS source with a Schottky injector would be comparable to fast electron beam lithography (EBL) systems.

### The electron impact gas ion source – test setup in NUS

The following sections will describe the test setup accomplished in NUS, on the electron impact gas ion source, towards a high brightness compact PBW system.

#### Focus ion beam (FIB) milling test of the source chip

The spacing between the upper and lower membranes in the prototype chip is about 1-2  $\mu$ m, which is limited by the bonding process. Chips produced via this method are not very reliable with risk of trapping particles between the two membranes and vacuum sealing failure. The ion source chip in our case is a modified generation, integrated on one single Si piece through many MEMS processes optimized by Delft. The spacing between the double-aperture (two membranes) is now less than 1  $\mu$ m. This 2<sup>nd</sup> generation chip is currently under test. We have carried out some inspections to check the gas feeding channel, and modified the bias connections in the chip. Metal layers (7 nm Cr + 7 nm Au) are coated by magnetic plasma on both sides of the chip before FIB milling.

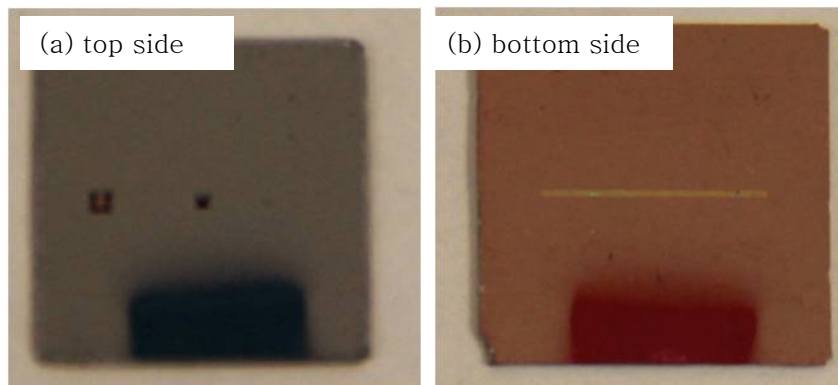


**Figure 12:** The miniature ion source chip 10 mm  $\times$  10 mm. a) the silicon side is opened with two windows by etching to reveal the top membrane. The left window is about 200  $\mu$ m for gas feeding into the channel. The right window is about 50  $\mu$ m for double aperture by FIB milling; b) the bottom membrane shows the confined channel between two membranes.

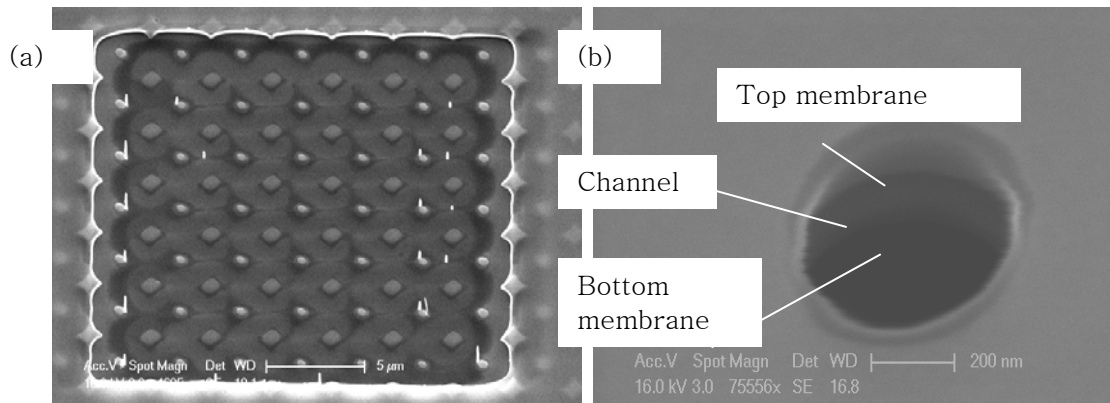


**Figure 13:** FE-SEM images of FIB milled membrane. a) gas feeding window at the 200  $\mu\text{m}$  window; b) double aperture at the 50  $\mu\text{m}$  window, taken using a Schottky emission SEM (Philips XL30)

One rectangle (20  $\mu\text{m} \times 10 \mu\text{m}$ ) at the 200  $\mu\text{m}$  window is created via top membrane removal by FIB. The opening in the channel for gas feeding to the double aperture is shown (Fig. 13a). A 500 nm double aperture is created in the 50  $\mu\text{m}$  window. With a 30 degree tilted angle, the channel between the two membranes is visible (Fig. 13b).

### SEM electron injector characterization

A Schottky emission SEM (Philips XL30) system is used at this stage for initial study. The ion current test setup is shown in Fig. 14. It consists of gas feed system, voltage feed through, chip holder and current measurement. Its electron beam current at different beam energy is studied first to estimate its impact to NAIS as electron injector, using a Faraday cup connecting to a picoammeter.

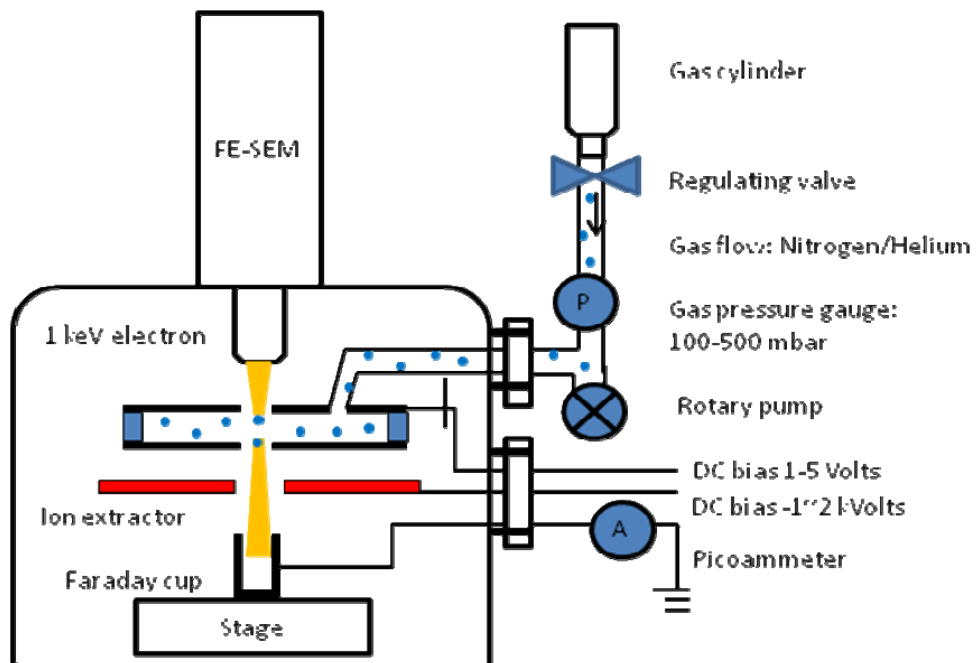


**Figure 14:** Schematics of experiment setup attached to a FESEM to characterize the electron impact gas ion source for PBW.

Due to the instrument limitation, this SEM provides an electron beam current of about 10-100 pA for 200 eV to 1 keV beam energy. Starting with helium and nitrogen we expect ion beam currents of a few pA.

### Gas dosing system and sample holder

The gas feeding system (Fig. 15) is vacuum sealed compatible to the SEM vacuum system. Built using Swagelok™ stainless steel tube and connector, the system can be pumped down to  $3 \times 10^{-2}$  mbar using an oil roughing pump. Nitrogen gas is feed in by adjusting the gas regulating valve and the gas inlet pressure is monitored by an Edwards

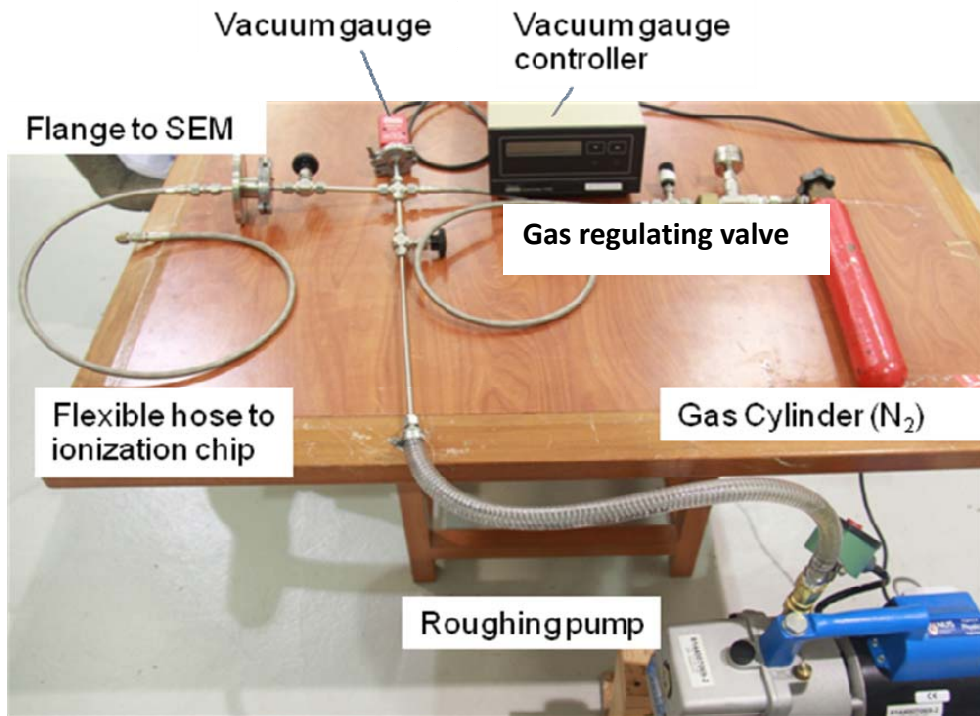


**Figure 15:** The gas feeding system.

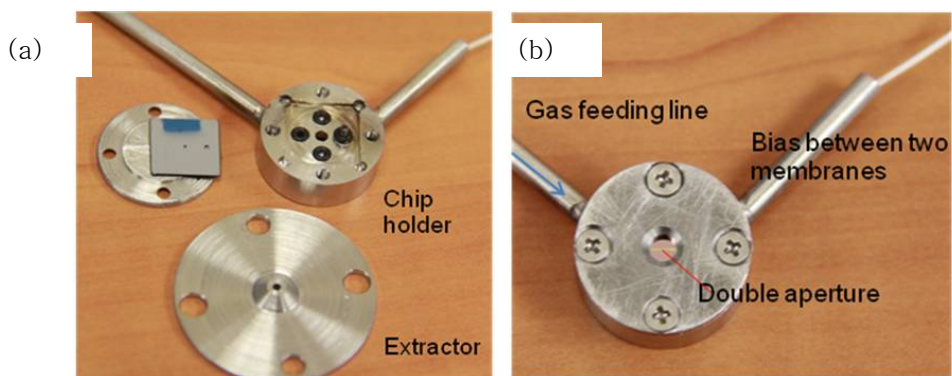


**Figure 16:** The holder and ion extractor for the miniature ion source chip. a) The source chip is loaded to a groove, supported with Viton o-rings. b) the chip is confined by screw. The bottom membrane and sealed channel is revealed, where the double aperture locates and ion extracted out.

PRM 10 vacuum gauge. The gas inlet pressure can be set from  $10^{-2}$  mbar to 1 bar. Various gas species can be dosed using this setup (He, N<sub>2</sub>, Ar), but modification should be taken for H<sub>2</sub> gas, especially at the roughing pump station for risk management.

The source chip is supported by o-rings to provide even pressure over the chip, preventing breaking the thin silicon nitride membrane. The O-ring also provides vacuum sealing for the gas feed into the 200  $\mu$ m window. The bias between the two membranes is to supply an electric field ( $\sim 10^6$  V/m) to push ions towards the extractor. This bias is supplied through a spring electrode to assure good electrical contact with the metal coated (7 nm Cr + 7 nm Au) membrane. This setup is designed for ion current test in the FESEM chamber, starting with nitrogen gas. With the gas feeding and the electron beam, the ions (N<sub>2</sub><sup>+</sup>, N<sup>+</sup>) are extracted and collected by the faraday cup, measured by a picoamp-meter (accuracy of 0.1 pA). The membrane bias can be adjusted via a 9 V battery. The extraction voltage can be varied from -1 kV up to -5 kV.

### Experimental setup with NAIS and FESEM

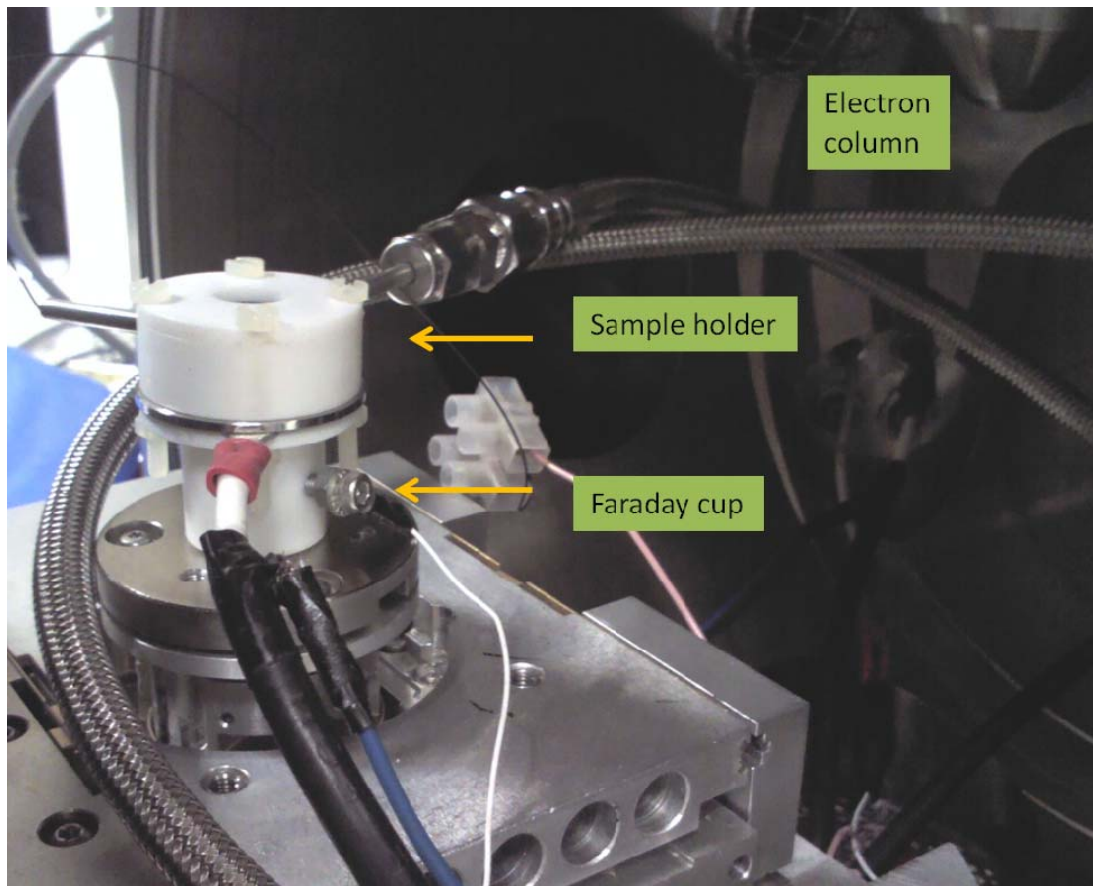


**Figure 17:** The holder and ion extractor with the NAIS chip mounted on the SEM stage (Singapore).

The NAIS chip with the sample holder was mounted on the FESEM stage, with gas feeding from the side flange and voltage feeding from a back flange. The electron beam from the FESEM is now injecting into the NAIS chip and ionizes gas feed into the system (Fig. 17).

By adjusting the gas regulating valve, nitrogen gas was fed into the NAIS chip

inside the SEM chamber, with inlet pressure from 1 mbar to 700 mbar. The SEM chamber remains at high vacuum level ( $6 \times 10^{-5}$  mbar). Therefore the gas dosing system is capable of gas dosing and vacuum proof. Due to the age of the SEM gun and its system limitation, the electron current is low (60-100 pA). Therefore, modification works are in process to increase the ion current measurement efficiency. Ion current output from this system will be tested in the future.

### Alternative Chip designs in Singapore

In Singapore alternative methods are being investigated to design the NAIS chip. Several approaches will be discussed in the next sections

#### Resist-based source chip design

Photoresist like SU-8 and PMMA have been widely used to fabricate microfluidic lab-on-chip devices, using lithography and resist bonding process [ 8 , 9 ]. Sealed microfluidic channels (50  $\mu\text{m}$  deep and 200  $\mu\text{m}$  wide) have been reported by SU-8 to SU-8 resist bonding [7]. The sealed channel was capable to take at least 1 atmosphere pressure drop. Shao et al. have demonstrated sealed microfluidic channel fabricated using PMMA[8].

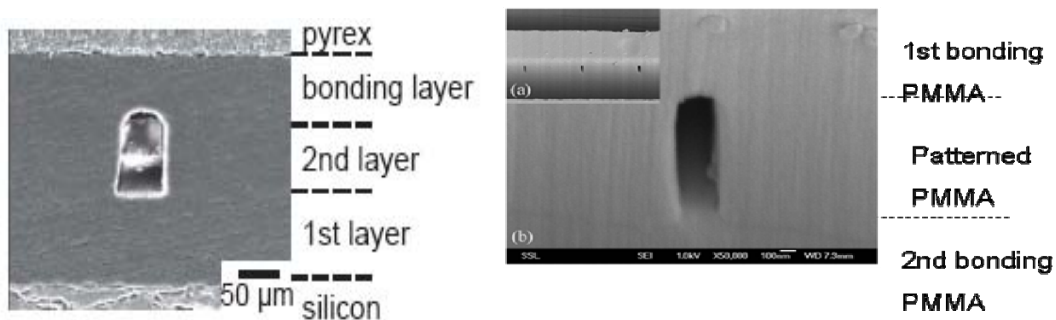


**Figure 18:** SEM image of the SU-8 and PMMA resist bonding. The bonding joint cannot be observed. Adapted from Ref.9.

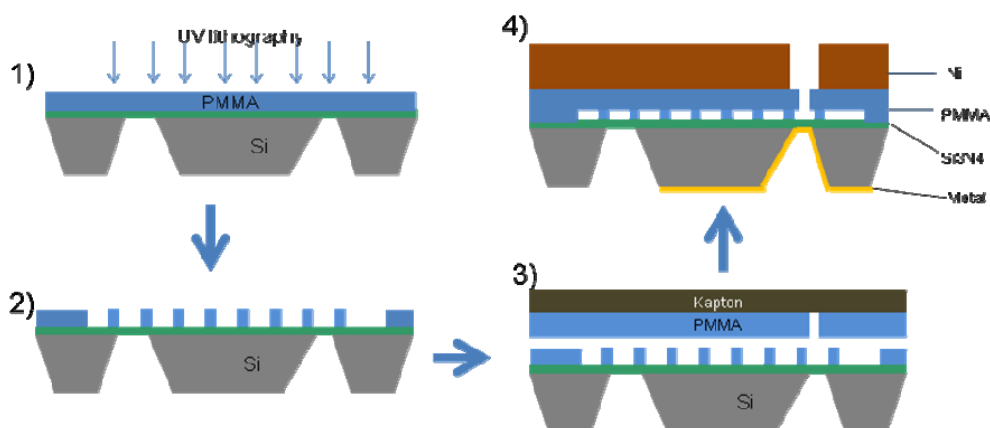


**Figure 19:** Proposed process to fabricate a PMMA bonding ion source chip. a) spin-coat 500 nm PMMA on pre-etched Si with silicon nitride membrane; b) UV pattern the channel in PMMA layer; c) pattern another PMMA on Kapton substrate; d) bond the two PMMA layers to form sealed channel. Peel off the Kapton layer. An additional Ni layer can be considered to function as the electrode layer and provide uniform pressure to fasten the chip in holder.

Therefore we propose to fabricate the source chip using SU-8 and PMMA for test. The advantage of PMMA bonding chip is that a Kapton layer (Fig. 19-3) can be removed easily. The nickel layer can be pre-patterned with exit for ions using UV lithography and electroplating (Fig. 19-4). This nickel layer can be used for the biasing between the two PMMA membranes, without additional metal deposition. Moreover, its thickness can be controlled from 100 nm to mm, which can conduct the heat away generated by electron back bombardment.

A SU-8 based gas ionization chip has been fabricated, in order to simplify the chip fabrication process and provide a reliable sealed gas feed system. A piece of glass was pre-cleaned by piranha etching ( $\text{H}_2\text{SO}_4 : \text{H}_2\text{O}_2 = 9 : 1$ ) and prebaked at  $200\text{ }^\circ\text{C}$  for 10 minutes. A  $5\text{ }\mu\text{m}$  thick layer of MicroChem SU-8 2005 resist was then spin-coated on the glass slide (at 3500 rpm). The resist was soft-baked at  $95\text{ }^\circ\text{C}$  for 2 minutes on hotplate, before UV exposure. After exposure the resist was post-baked  $95\text{ }^\circ\text{C}$  for 3 minutes and then developed. Pattern structures (micro-channel with reservoirs) from the UV mask were transferred to the resist. Another  $5\text{ }\mu\text{m}$  thick layer of SU-8 was spin-coated on a  $50\text{ }\mu\text{m}$  thick PMMA sheet, follows by soft-bake. Both the SU-8 samples were heated at  $95\text{ }^\circ\text{C}$  for 3 minutes. The SU-8 to SU-8 bonding was performed by cover the SU-8/glass sample with SU-8/PMMA sample, maintaining the temperature at  $95\text{ }^\circ\text{C}$ . The SU-8 resist were close to the glass-point at this step. The resist reflowed and gentle bonding was formed. The samples were then transferred to UV exposure (over-dosage exposure). The two SU-8 layers were well bonded by molecular cross-linking.

To test the SU-8 2005 resist bonding, the sealed channel was opened at a reservoir by punching through the top PMMA/SU-8 layers. Air was forced into the channel by using a syringe. The sealed channel was able to take a pressure difference of about 1 atmosphere without observation of resist peeling off or breaking between the two resist layers. To further reduce the resist thickness, the SU-8 2005 resist can be diluted with solvent (MicroChem SU-8 thinner) to achieve layer thickness  $< 500\text{ nm}$ . The glass substrate can be changed to Si or PMMA, which have better adhesion with SU-8 than glass. The SU8 layer on PMMA sheet can be pre-patterned using UV lithography before thermal bonding. The double-aperture can be created similarly using FIB milling, to function as an ion source ionization chamber.

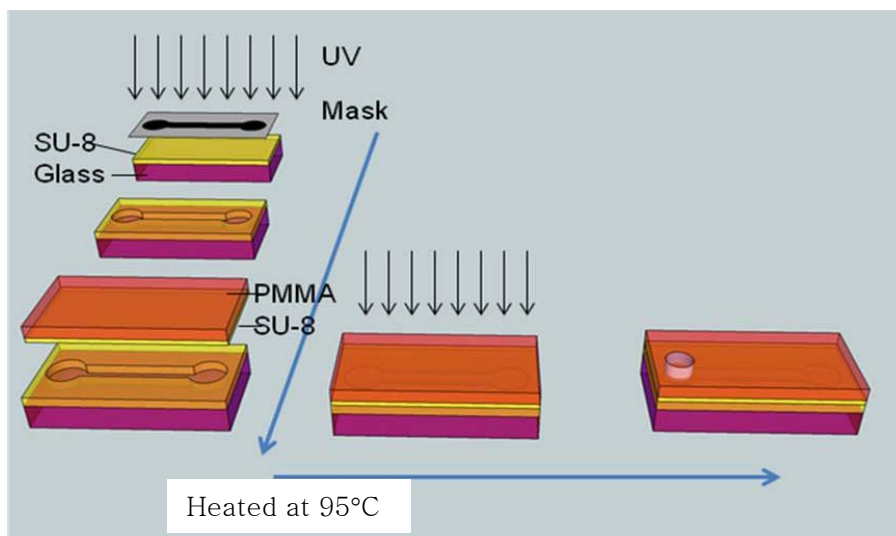


**Figure 20:** Prepare the SU8 bonding chip using UV exposure and thermal heating.

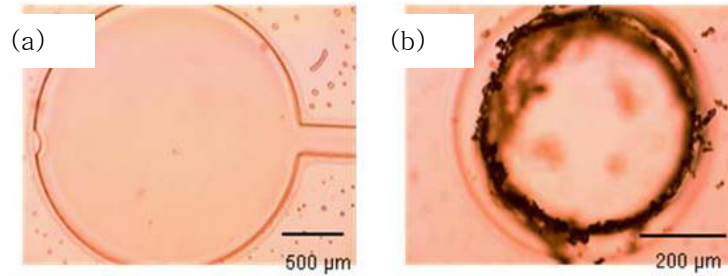


**Figure 21:** Optical images of a) the reservoir of the sealed channel; b) hole pouched through the PMMA and SU8 layer at the reservoir to introduce gas.

### Proton beam fabricated source chip design

We are currently developing a method to fabricate a miniature source chip using proton beam irradiation of Si which has the advantage of a higher strength compared to polymer chips. Proton beam irradiation has been reported with the capability to fabricate 3-D structures and buried channels in Si wafer [10].

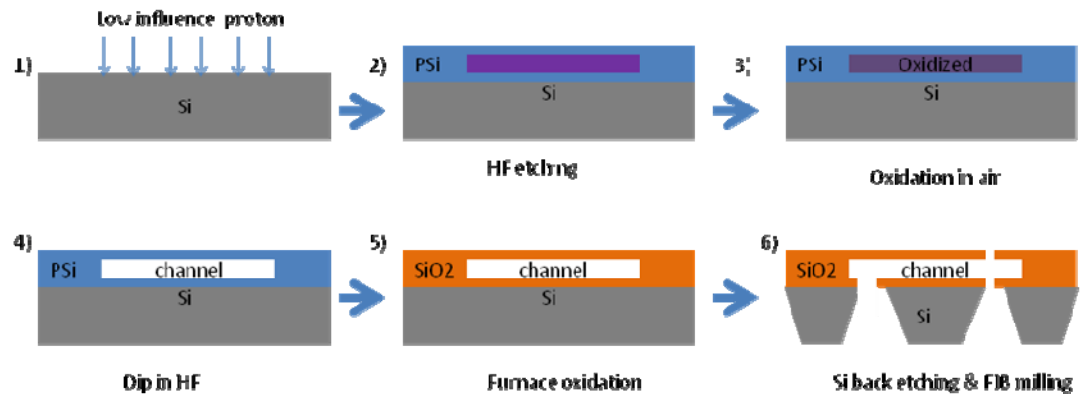


**Figure 22:** Proposed process to fabricate a miniature ion source on a single Si chip using proton beam irradiation. 1) Si wafer is irradiated using low dosage proton irradiation; 2) the Si chip undergoes hydrogen fluoride ( HF) etching in an electric potential across the Si chip. Porous Si (PSi) is formed on top; 3) the Si chip is left in air for few days to oxidize the proton irradiated area; 4) the Si chip is dip into HF and channel is formed as the oxidized Si is dissolved; 5) The top PSi layer is oxidized to form glass during furnace heating; 6) the chip is etched from the back. Gas inlet and double aperture can be milled using FIB.

By tuning the proton dosage and energy, the channel depth and the PSi layer thickness can be tuned ranging from 100 – 500 nm. Therefore, it is interesting to fabricate a NAIS chip with thin membranes and small spacing (100 nm). We are currently working with Prof. Mark Breese (CIBA, NUS) and his team to develop a suitable procedure and establish preliminary test chips.

## **Results and Discussion:**

Initial test in Delft have shown high brightness for the old electron impact chip design. The new chip design has potentially higher brightness but is still under investigations and will be tested in more detail.

In the coming months we plan to work on the following points:

- 1) Optimize the current RF ion source system in CIBA using the developed ion source test bench. The electronics for this system will be upgraded to allow the system to run at 200 kV. This system will initially be tested at 5 kV. It will be designed to be compatible with higher energies of up to 200 kV.
- 2) The NAIS test set up will be further implemented to obtain ion current measurement. Several gas species (N<sub>2</sub>, Ar, Helium and H<sub>2</sub>) as well as several NAIS chip designs will be tested .
- 3) The brightness and energy spread measurement tools will be developed and tested. Ion source brightness tests will be carried out both for NAIS and FR sources.

Since the system is still under development we have been studying different designs. At the 3 Beams conference the work on the design of the new electron impact ion source was selected as an invited poster. We are currently preparing a paper on this work which we plan to submit to JVSTB. The PI has also published several papers based on earlier grants from the US air force: **AOARD 07-4017, AOARD 06-4004 & AOARD 05-4037**

## **Journal Publications:**

- 1) Injector evaluation in an electron impact ion source for high brightness proton beam writing, Nannan. Liu <sup>1,a)</sup>, David S. Jun<sup>2)</sup>, Cornelis W. Hagen, Pieter Kruit<sup>2)</sup> P. Santhana Raman<sup>1)</sup> and Jeroen A. van Kan, In preparation
- 2) Resist Evaluation for Proton Beam Writing, Ni mold Fabrication and Nano-replication Y.H. Wang, P. Malar, \*J.A. van Kan, submitted to microsystem technologies.
- 3) Orthogonal and fine lithographic structures attained from the next generation proton beam writing facility, Yao Yong, Santhana Raman P, \*van Kan JA, submitted to microsystem technologies.
- 4) Preliminary lithographic structures attained from the next generation proton beam writing facility, Yao Yong, P. Santhana Raman, J.A. van Kan, Submitted JVSTB
- 5) Improved beam spot measurements in the 2<sup>nd</sup> generation proton beam writing system, Yao Yong<sup>a)</sup>, Martin W. van Mourik<sup>b)</sup>, P. Santhana Raman<sup>a)</sup> and Jeroen A. van Kan, Nuclear Instruments & Methods in Physics Research Section B 306 (2013) 265-270.
- 6) High throughput fabrication of disposable nanofluidic lab-on-chip devices for single molecule studies, JA van Kan, C. Zhang, P. Malar and J.R.C. van der Maarel, Biomicrofluidics **6** (2012) 036502-1, 036502-9
- 7) The second generation Singapore high resolution proton beam writing facility, J.A. van Kan, P. Malar, and Armin Baysic de Vera, Review of Scientific Instruments **83** (2012) 02B902-1 02B902-3.
- 8) The Singapore high resolution single cell imaging facility, Frank Watt, Xiao Chen, Armin Baysic De Vera, Chamika C N Udalagama, Ren Minqin, Jeroen A van

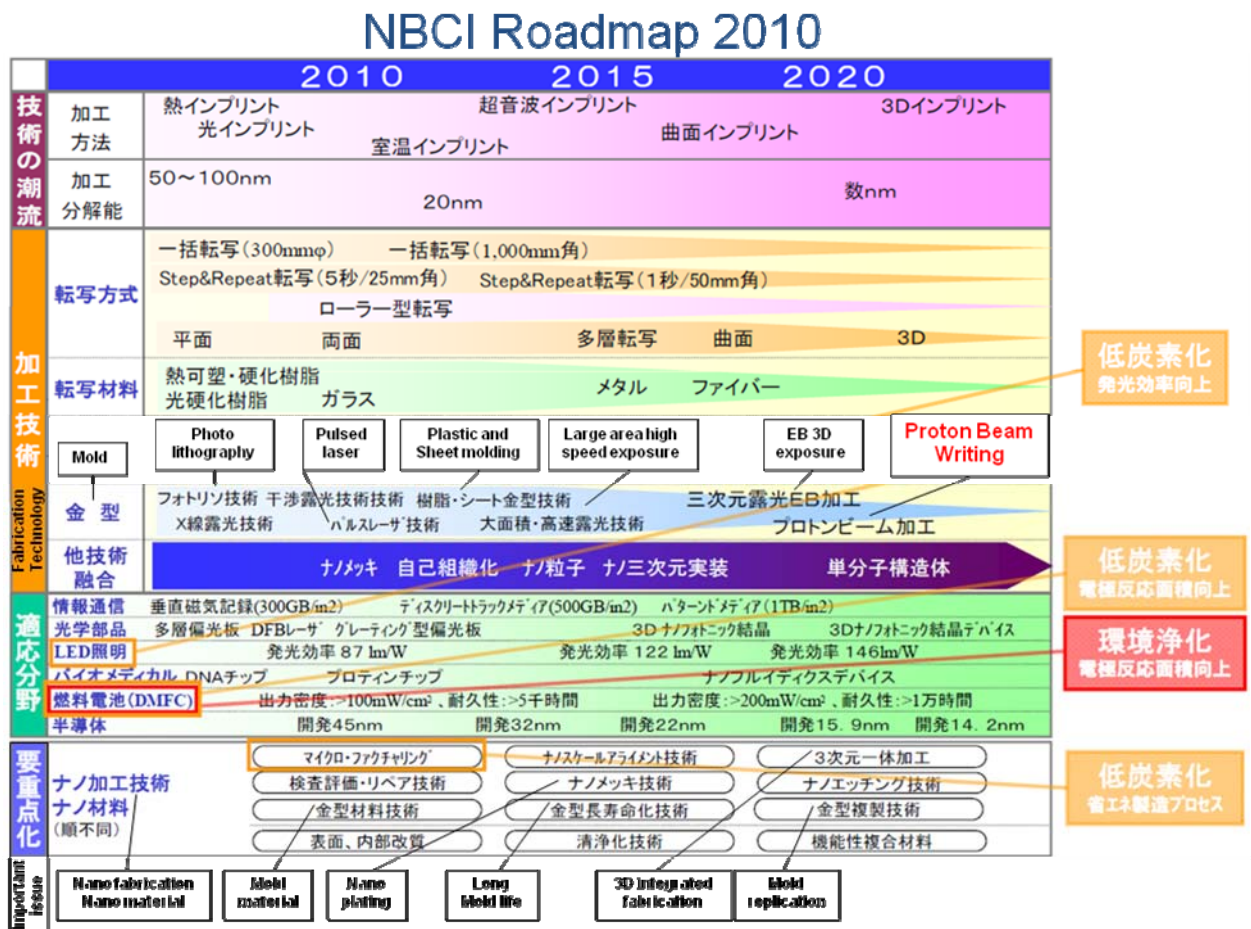
- Kan, Andrew A Bettiol, Nuclear Instruments & Methods in Physics Research Section **B** *in press*.
- 9) Proton beam writing nanoprobe facility design and first test results, J.A. van Kan, P. Malar, Armin Baysic de Vera, Xiao Chen, A.A. Bettiol and F. Watt, Nuclear Instruments & Methods in Physics Research Section **A** **645** (2011) 113-115.
  - 10) Proton Beam Writing a platform technology for high quality three-dimensional metal mold fabrication for nanofluidic applications, J.A. van Kan, P.G. Shao, Y.H. Wang and P. Malar, Microsystem Technologies **17** (2011) 1519-1527.
  - 11) Exposure parameters in proton beam writing for KMPR and EPO Core negative tone photoresists, M.D. Ynsa, P. Shao, S.R. Kulkarni, N.N. Liu, J.A. van Kan, Nuclear Instruments & Methods in Physics Research Section **B** **269** (2011) 2409–2412

### **Conference Organization/presentations:**

1. **Invited talk** at the 10<sup>th</sup> International Workshop on High Aspect Ratio Micro and Nano System Technology (HARMNST 2013 Workshop) in Berlin, 21-24 April 2013 (~200 participants). Title “*Proton Beam Writing: A Tool for High Aspect Ratio Resist Patterning and Nanoimprint Lithography*”.
2. Poster presentation at HARMNST 2013 Title ”*Resist Evaluation for Proton Beam Writing Ni mold Fabrication and Nano-replication*”
3. **Session Chair of two sessions** at the 22<sup>nd</sup> International Conference on the Application of Accelerators in Research and Industry (5 – 10 August 2012, Fort Worth, Texas, USA, CAARI has over 500 participants).
4. **Two Invited review presentation: 2012**, 22<sup>nd</sup> International Conference on the Application of Accelerators in Research and Industry (5 – 10 August 2012, Fort Worth, Texas, USA), Title: 1) *Precise mold fabrication using proton beam writing for Cell and DNA manipulation*. 2) *Next Generation MeV Proton Beam Focusing; What is required for sub 10 nm 3D lithography?*
5. **Invited Oral presentation: 2012** International Conference on Nuclear Microprobe Technology and applications (Lisbon, Portugal). Title: *The 2<sup>nd</sup> Generation Proton Beam Writing Facility; Results and Outlook*.
6. Invited poster presentation at the the 56<sup>th</sup> International Conference on Electron, Ion and Photon Beam Technology & Nanofabrication, 28 May – 1 June 2011, Hawaii, USA. Title: *Electron impact gas ion source development; evaluation of different electron injection sources*, N. Liu, J.A. van Kan, D. Jun, C.W. Hagen, P. Kruit.
7. Oral presentation: at the the 56<sup>th</sup> International Conference on Electron, Ion and Photon Beam Technology & Nanofabrication, 28 May – 1 June 2011, Hawaii, USA. Title *First Lithography results obtained with the 2<sup>nd</sup> generation MeV proton beam writing facility*.
8. 2011 **Chair of section BB** of the International Conference on Materials for Advanced Technologies ICMAT 26/06/11–1/07/11, Singapore (ICMAT 2700 participants).
9. **Invited Oral presentation: 2011** February at the Ion-beam Induced Nanopatterning of Materials, Bhubaneswar, India. Title *Nickel injection mould fabrication via proton beam writing and UV lithography for fluidic chip applications*
10. **Invited Oral presentation: 2010** July at the 8<sup>th</sup> Charged Particle Optics conference, Singapore. Title *Proton beam nano-probe technology and applications*

11. Oral presentation: June 2011 at the International Conference on Materials for Advanced Technologies 26/06/11 – 1/07/11, Singapore. Title *Next Generation Proton Beam Nano-probe Technology for Proton Beam Writing*.
12. Poster presentation at 36<sup>th</sup> MNE conference, September 2010, Genoa, Italy On “*Mold fabrication using PBW for nano fluidic and DNA analysis*”
13. Poster presentation at ICNMTA, July 2010, Leipzig Germany. On “*The Singapore next generation proton beam writing facility*”. This poster got an honourable mentioning at the conference.

## Appendix 1



**Publications:** See attached zip file.

## References:

---

- 1 *Ion beam lithography and nanofabrication: A review*, F. Watt, A.A. Bettiol, J.A. van Kan, E. J. Teo and M.B.H. Breese, **IJN 4**, (2005), 269
- 2 *The National University of Singapore high energy ion nano-probe facility: Performance tests*, F. Watt, J.A. van Kan, I. Rajta 1, A.A. Bettiol, T.F. Choo, M.B.H. Breese, T. Osipowicz, Nuclear Instruments and Methods in Physics Research **B 210** (2003) 14–20.
- 3 Proton Beam Writing of 3D Nanostructures in Hydrogen SilsesQuioxane J.A. van Kan, A.A. Bettiol and F. Watt, *Nano letteres* **6**, (2006), 579.
- 4 *The second generation Singapore high resolution proton beam writing facility*, J.A. van Kan, P. Malar, and Armin Baysic de Vera, Review of Scientific Instruments **83** (2012) 02B902-1 02B902-3.
- 5 M. van der Heijden, MSc thesis, Charged particle optics group, TU Delft (2011).
- 6 D. Jun and P. Kruit, *J. Vac. Sci. Technol. B* **29**, 06F603 (2011).
- 7 P. Kruit, M. Bezuijen and J. E. Barth, *J. Appl. Phys.* **99**, 024315 (2006).
- 8 R. J. Jackman, T. M. Floyd, R. Ghodssi, M. A. Schmidt and K. F. Jensen, *J. Micromech. Microeng.* **11**, 263–9 (2001).
- 9 P. G. Shao, J.A. Van Kan, L.P. Wang, K. Ansari, A.A Bettol, F. Watt,, *Applied Physics Letters* **88** , 093515 (2006).
- 10 S. Azimi, Z. Y. Dang, J. Song, M. B. H. Breese, E. Vittone and J. Forneris, , *Applied Physics Letters* **102**, 042102 (2013).